

Time-Domain Finite-Element Simulation of Three-Dimensional Scattering and Radiation Problems Using Perfectly Matched Layers

D. Jiao¹, J. M. Jin¹, E. Michielssen¹, and D. Riley²

¹Center for Computational Electromagnetics
Department of Electrical and Computer Engineering
University of Illinois at Urbana-Champaign
Urbana, Illinois 61801-2991

²Electromagnetics and Plasma Physics Analysis Department
Sandia National Laboratories
Albuquerque, New Mexico 87185-1152

1 Introduction

Perfectly matched layers (PMLs) [1] are often used to implement absorbing boundary conditions (ABCs) in the finite-difference time-domain (FDTD) and finite-element frequency-domain (FEFD) simulations of open-region wave propagation problems. In this paper, we develop a PML scheme for mesh truncation in the finite-element time-domain analysis of three-dimensional (3D) open-region electromagnetic scattering and radiation phenomena. The proposed algorithm can support nonconstant PML parameters within each element, which facilitates the efficient utilization of higher-order vector basis functions.

2 Formulation

Consider the problem of modeling the electric field $\mathbf{E}(\mathbf{r}, t)$ generated by $\mathbf{J}(\mathbf{r}, t)$ in the presence of an object, with both the source and the object residing in a region V_i . To formulate a finite-element scheme that permits the computation of $\mathbf{E}(\mathbf{r}, t)$, a PML is introduced outside V_i to truncate the computational domain (Fig. 1). The union of the PML region and V_i is denoted V_o . The surfaces bounding V_i and V_o are denoted by S_i and S_o , respectively. In the PML region, a conductivity σ_x is specified for the PML walls perpendicular to the x axis; similarly, conductivities σ_y and σ_z are specified for the PML walls perpendicular to the y and z axes, respectively. Inside the PML, the field satisfies the following second-order vector wave equation

$$\epsilon\bar{\Lambda}(\mathbf{r}, t) \star \partial_t^2 \tilde{\mathbf{E}}(\mathbf{r}, t) + \nabla \times (\mu\bar{\Lambda})^{-1}(\mathbf{r}, t) \star \nabla \times \tilde{\mathbf{E}}(\mathbf{r}, t) = 0 \quad (1)$$

where \star stands for temporal convolution, $\tilde{\mathbf{E}}(\mathbf{r}, t)$ denotes the stretched electric field [2] given by

$$\tilde{\mathbf{E}}(\mathbf{r}, t) = \left[\left(1 + \frac{\sigma_x}{\epsilon} \partial_t^{-1}\right) E_x(\mathbf{r}, t), \left(1 + \frac{\sigma_y}{\epsilon} \partial_t^{-1}\right) E_y(\mathbf{r}, t), \left(1 + \frac{\sigma_z}{\epsilon} \partial_t^{-1}\right) E_z(\mathbf{r}, t) \right]^T \quad (2)$$

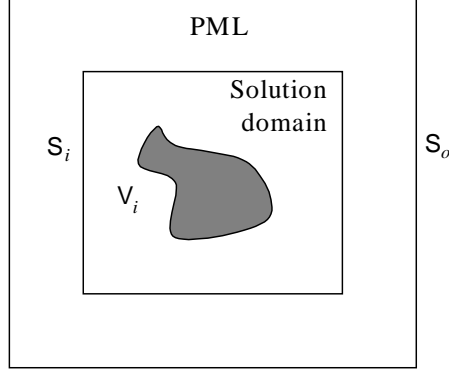


Figure 1: Illustration of solution domain truncated by PML.

with ∂_t^{-1} denoting temporal integration, and $\bar{\Lambda}(\mathbf{r}, t)$ is the time-domain counterpart of the diagonal tensor

$$\bar{\Lambda} = \hat{x}\hat{x} \left(\frac{S_y S_z}{S_x} \right) + \hat{y}\hat{y} \left(\frac{S_x S_z}{S_y} \right) + \hat{z}\hat{z} \left(\frac{S_x S_y}{S_z} \right) \quad (3)$$

in which S_ξ ($\xi = x, y, z$) are the stretching variables given by

$$S_\xi = 1 + \frac{\sigma_\xi}{j\omega\epsilon_0} \quad \xi = x, y, z. \quad (4)$$

To seek the TDFEM solution of (1), we employ Galerkin's method to convert (1) into a matrix equation. Assuming a Dirichlet boundary condition on S_o , the weak-form solution satisfies

$$\iiint_{V_o} \{ \epsilon \mathbf{N}_i(\mathbf{r}) \cdot \bar{\Lambda}(\mathbf{r}, t) \star \partial_t^2 \tilde{\mathbf{E}}(\mathbf{r}, t) + \nabla \times \mathbf{N}_i(\mathbf{r}) \cdot (\mu \bar{\Lambda})^{-1}(\mathbf{r}, t) \star \nabla \times \tilde{\mathbf{E}}(\mathbf{r}, t) + \mathbf{N}_i(\mathbf{r}) \cdot \partial_t \mathbf{J}(\mathbf{r}, t) \} dV = 0 \quad (5)$$

where $\mathbf{N}_i(\mathbf{r})$ denotes the vector basis function. Expanding the stretched electric field as

$$\tilde{\mathbf{E}}(\mathbf{r}, t) = \sum_{j=1}^N u_j(t) \mathbf{N}_j(\mathbf{r}) \quad (6)$$

with N denoting the total number of expansion functions, and assuming that conductivities σ_x , σ_y , and σ_z are constant within each element, the following ordinary differential equation is derived

$$\sum_{e=1}^M \left(\mathbf{T}^e \frac{d^2 u}{dt^2} + \mathbf{T}_p^e \frac{du}{dt} + \mathbf{T}_q^e u + \mathbf{S}^e u + \sum_{\xi=x,y,z} \mathbf{S}_\xi^e \psi_\xi + \sum_{\xi=x,y,z} \mathbf{T}_\xi^e \psi_\xi + f^e \right) = 0. \quad (7)$$

Here, M denotes the total number of finite elements, \mathbf{T}^e , \mathbf{T}_p^e , \mathbf{T}_q^e , \mathbf{S}^e , \mathbf{S}_ξ^e , and \mathbf{T}_ξ^e ($\xi = x, y, z$) are square matrices whose expressions can be identified from (5), $u = [u_1, u_2, \dots, u_N]^T$ is the unknown vector, f^e is the excitation vector, and ψ_ξ ($\xi = x, y, z$) are vectors that can be expressed as

$$\psi_\xi(t) = \sigma_\xi / \epsilon e^{-\sigma_\xi t / \epsilon} \bar{u}(t) \star u(t) \quad \xi = x, y, z \quad (8)$$

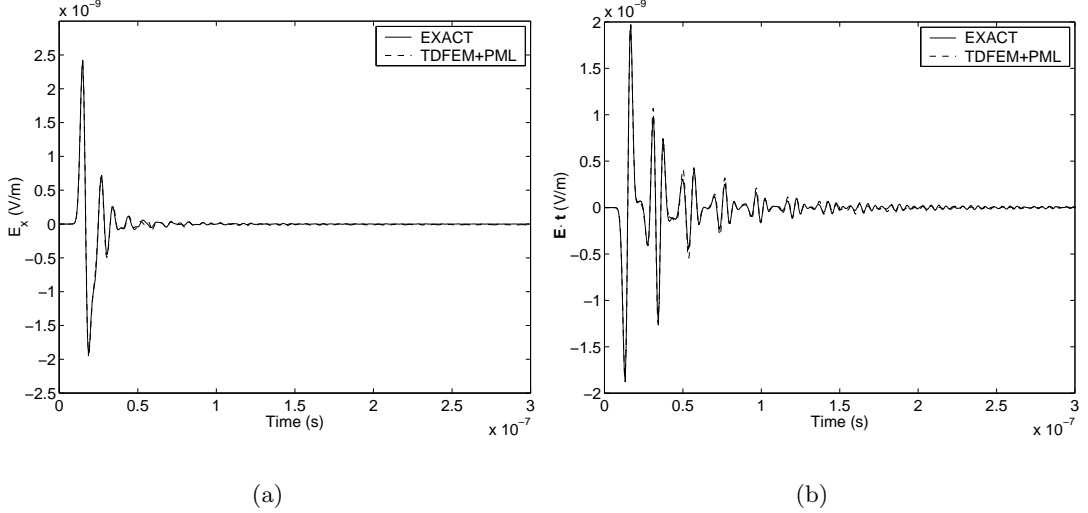


Figure 2: Scattering from a dielectric sphere of radius 0.47 m and a relative permittivity 8.0. (a) Electric field E_x at $\mathbf{r} = 0.71\hat{\mathbf{x}} + 0.31\hat{\mathbf{y}} - 0.22\hat{\mathbf{z}}$ m (The normalized RMS error is 0.79%). (b) Electric field $\mathbf{E} \cdot \mathbf{t}$ at $\mathbf{r} = 0.0035\hat{\mathbf{x}} - 0.003\hat{\mathbf{y}} - 0.67\hat{\mathbf{z}}$ m with $\mathbf{t} = 0.97\hat{\mathbf{x}} + 0.22\hat{\mathbf{y}} - 0.056\hat{\mathbf{z}}$ (The normalized RMS error is 1.2%).

in which $\bar{u}(t)$ denotes the unit step function. The above convolution can be recursively evaluated as described in [3] without the need to store fields of all past time steps. Second-order accuracy is ensured by adopting a linear interpolation for the fields within each time step.

The assumption used in deriving (7) that σ_ξ ($\xi = x, y, z$) be constant within each element can be removed although the formulation is more involved. It then remains to choose the proper spatial and temporal discretization schemes. For the spatial discretization, the unknown fields can be expanded using edge elements, higher-order edge elements, or orthogonal vector basis functions. For the temporal discretization, we can employ the central difference scheme, the backward difference scheme, and the Newmark method. In this work, both zeroth- and higher-order vector elements are used to expand the unknown field. The Newmark method is employed for temporal discretization.

3 Numerical Examples

An example considered here is a dielectric sphere of radius 0.47 m. The PML has a thickness of 0.3 m, and is placed 0.5 m away from the surface of the dielectric sphere. The computational domain is divided into 2,633 tetrahedra, yielding 15,556 unknowns with the use of the first-order vector basis functions. The incident pulse is a Neumann pulse with a maximum incident frequency of 600 MHz. The calculated electric fields at $\mathbf{r} = 0.71\hat{\mathbf{x}} + 0.31\hat{\mathbf{y}} - 0.22\hat{\mathbf{z}}$ m and $\mathbf{r} = 0.0035\hat{\mathbf{x}} - 0.003\hat{\mathbf{y}} - 0.67\hat{\mathbf{z}}$ m are shown in Fig. 2. The proposed TDFEM–PML scheme correctly characterizes the multiple interactions among the multiply reflected and creeping waves. The simulation results agree very well with the theoretical data.

Next, we simulate a conducting cube with a side-length of 1 m. The PML is of thickness 0.3 m, and is placed 0.5 m away from the conducting surface. The Neumann

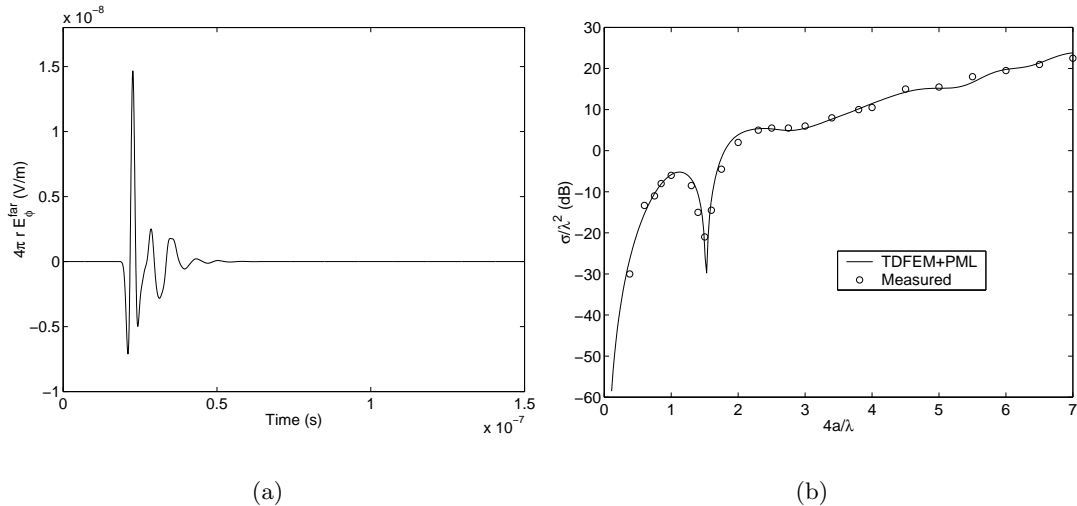


Figure 3: (a) Backscattered far-field $4\pi r E_{\phi}^{\text{far}}$ versus time. (b) Backscatter RCS versus the electrical size of the conducting cube ($a = 1$ m).

pulse is normally incident upon the cube. The entire computational domain is subdivided into 6,278 tetrahedra, yielding 42,994 unknowns with the use of first-order vector basis functions. The calculated far-field temporal signature is shown in Fig. 3(a) and the backscatter RCS is plotted in Fig. 3(b) versus the electrical size of the cube. The numerical simulation agrees very well with the measured data.

4 Conclusion

This paper presented an algorithm for realizing PMLs in the TDFEM-based simulation of 3D open-region electromagnetic scattering and radiation problems. The formulations are based on the vector wave equation in an anisotropic and dispersive medium. By allowing for the variation of the PML parameters within each finite element, the proposed algorithm can also make efficient use of higher-order vector basis functions. Numerical examples demonstrated that the proposed PML algorithm is sufficiently accurate and constitutes a viable alternative to the boundary integral-based schemes for the mesh truncation of open-region scattering and radiation problems.

References

- [1] J. Berenger, "A perfectly matched layer for the absorption of electromagnetic waves," *J. Comput. Phys.*, vol. 144, no. 2, pp. 185–200, 1994.
- [2] W. C. Chew and W. Weedon, "A 3D perfectly matched medium from modified Maxwell's equations with stretched coordinates," *Microwave Opt. Tech. Lett.*, vol. 7, no. 13, pp. 599–604, 1994.
- [3] D. Jiao and J. M. Jin, "Time-domain finite element modeling of dispersive media," *IEEE Microwave Wireless Comp. Lett.*, vol. 11, pp. 220–223, May 2001.